ELSEVIER

10 January 1997

Chemical Physics Letters 264 (1997) 371–375

CHEMICAL PHYSICS LETTERS

Ab initio molecular orbital model of scanning tunneling microscopy. Benzene and benzene adsorbed on a Ag surface

M. Hidaka [a], T. Fujita [a], H. Nakai [a], H. Nakatsuji [a,b,*]

[a] *Department of Synthetic Chemistry and Biological Chemistry, Faculty of Engineering, Kyoto University, Sakyo-ku, Kyoto 606-01, Japan*
[b] *Institute for Fundamental Chemistry, 34-4 Tanaka Nishi-Hiraki-cho, Sakyo-ku, Kyoto 606, Japan*

Received 2 October 1996; in final form 28 October 1996

Abstract

The molecular orbital (MO) model of scanning tunneling microscopy (STM) developed previously is applied to the Pd_2 tip C_6H_6 sample system to examine the effect of tilting the tip, and to benzene adsorbed on a silver surface to investigate the effect of the surface–adsorbate interaction on the STM image. The effect of tilting the tip is shown to depend on the nature of the tip MOs responsible for the STM current. The possibility of elucidating the site and geometry of the adsorbate by a combined use of experimental and theoretical STM images is discussed.

1. Introduction

Scanning tunneling microscopy (STM), developed by Binnig et al. [1], is now widely used not only for observing surface–adsorbate systems, but also as a tool for manipulating the surface on an atomic scale [2,3]. Despite its promising usefulness, however, detailed mechanisms of STM, such as the reality of the STM image, and the electronic processes in surface manipulations, have not yet been fully understood. Tsukada and co-workers developed a theory of the STM image based on Bardeen's perturbation theory [4] using a first-principles density functional approach [5,6]. They also presented a theoretical model dealing with atomic manipulation by STM [7,8]. We have proposed an ab initio molecular orbital (MO) model of STM using Hartree–Fock (HF) theory and including the effect of electron correlation [9]. Based on these theories, it has now become clear that the STM image does not necessarily represent the arrangement of surface atoms but the local electronic structures of the tip–sample systems [10–13].

We show in this study that our MO model of STM is useful for understanding the detailed implications of STM images. We study the STM image of benzene, analyzing the effect of tilting the tip and the effect of the metal surface on which benzene is adsorbed.

2. Calculational method

The MO model of STM has been presented in detail in Ref. [9]. The STM image is drawn theoreti-

* Corresponding author.

PII S0009-2614(96)01349-8

cally as a contour map of the square of the transition matrix, $|M_{m\to n}|^2$, which is given in HF theory as

$$M_{m\to n} = \langle \Psi^{CT}_{m\to n}|\hat{H}|\Psi_0\rangle = \sqrt{2}\left[\langle \phi^T_n|\hat{h}|\phi^S_m\rangle + \sum_k^{N_S+N_T}\left(\langle \phi^T_n\phi_k|\phi^S_m\phi_k\rangle - \langle \phi^T_n\phi_k|\phi_k\phi^S_m\rangle\right)\right], \quad (1)$$

where S and T denote the sample and tip, and m and n denote their MOs, respectively: the electron flows from MO m to MO n. The first term is the one-electron integral, and the second and third are the two-electron Coulomb and exchange terms in which ϕ_k are the MOs of both the sample and the tip. N_S and N_T denote the number of MOs of the isolated sample and tip.

We calculated two tip–sample systems, Pd_2–C_6H_6 and Pd_2–C_6H_6/Ag_4. The geometrical parameters for Pd_2, a square Ag_4 cluster [14] and C_6H_6 [15] were fixed at the experimental values and the

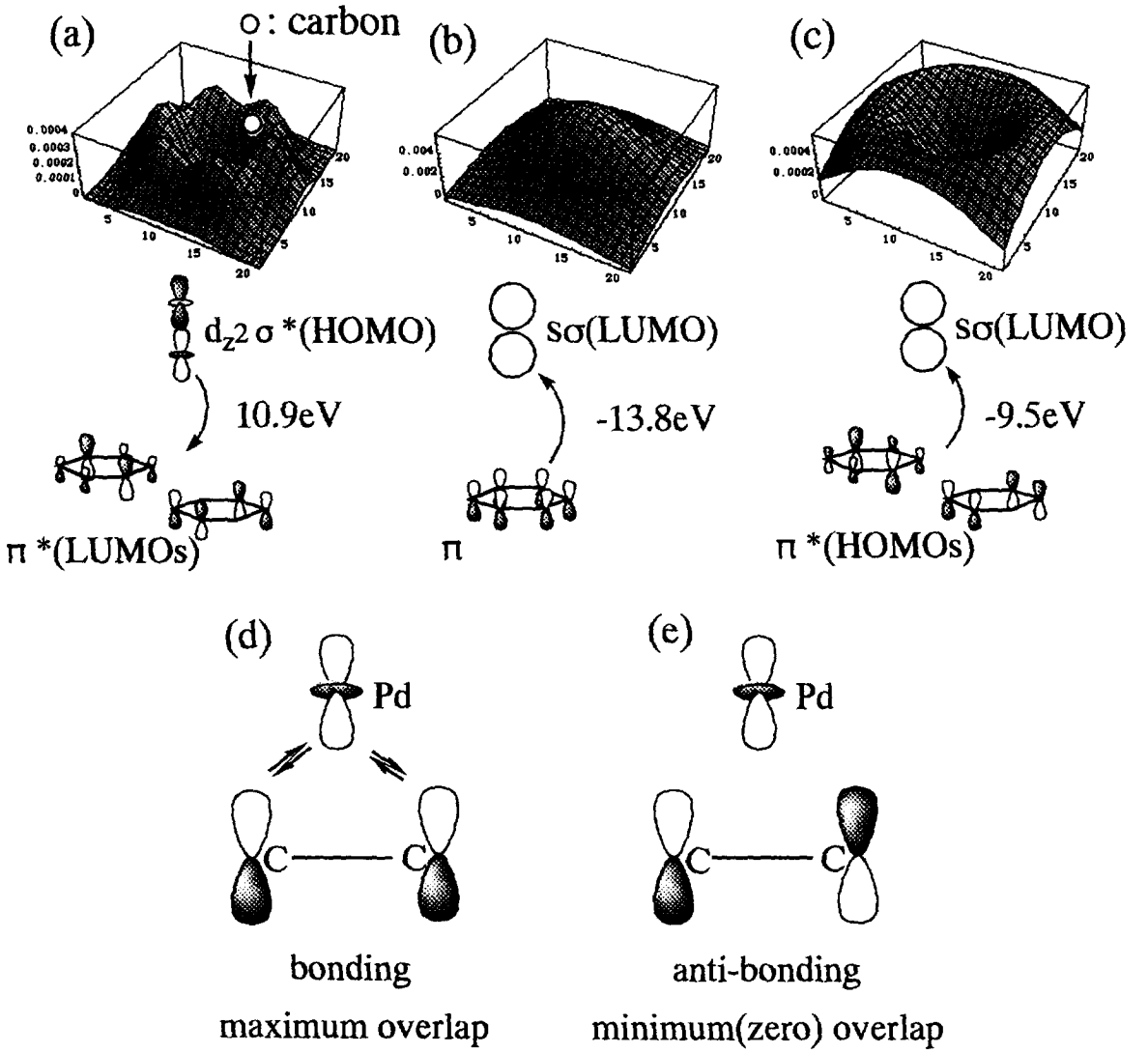

Fig. 1. (a–c) Calculated STM images of benzene. The molecular orbitals responsible for these images and the bias voltage are shown below the images. (d,e) Maximum and minimum overlap between the sample and the tip orbitals.

distance between the Ag_4 cluster and the aromatic ring was fixed at 2.3 Å, a theoretical value [16]. The sample–tip separation was fixed at 3 Å throughout the scanning, which corresponds to the experimental constant-height mode.

The Gaussian basis sets used for Pd and Ag were (3s3p4d)/[3s2p2d] and (3s3p4d)/[2s1p1d] sets, respectively, and the Kr cores were replaced by the relativistic effective core potentials [17]. For carbon and hydrogen, we used the Huzinaga–Dunning (9s5p)/[4s2p] and (4s)/[2s] sets, respectively [18,19]. The HF calculations were performed using HONDO8 [20] software.

3. Tilting of the Pd_2 tip on the C_6H_6 sample

We have reported previously the theoretical STM image for the Pd_2–C_6H_6 system [9]. Here we report a more detailed analysis of this system, especially the effect of tilting the Pd_2 tip on the C_6H_6 sample. Fig. 1 shows the calculated STM image of this system for the vertical tip geometry. These images correspond to the particular transitions between the sample and the tip orbitals. We define a positive bias voltage when an electron current flows from the tip to the sample: in Fig. 1a, the current flows from the tip to the sample and in Figs. 1b and 1c in an opposite direction. Fig. 1d shows the largest overlap between the molecular orbitals of the tip and the sample C–C bond, while Fig. 1e shows the smallest overlap.

In Fig. 1a, the overlap between the tip $d_{z^2}\sigma^*$ MO and the benzene degenerate π^* MOs decreases in the middle of the C–C bond and on the center of the aromatic ring, so that each carbon atom of the aromatic ring can be seen separately. Note that the position of the carbon nucleus is inside each hill; the top of the hill is on each C–H bond. In Figs. 1b and 1c, the overlap becomes large on the C–C bond and in Fig. 1b further at the center of the aromatic ring, so that the STM image makes a mound in Fig. 1b, while a doughnut is formed in Fig. 1c, the size being larger than that of the aromatic ring of the carbons.

The bias voltage applied here to get these images is higher than that in a usual STM experiment. The benzene molecule alone is an insulator having a large HOMO–LUMO gap. Thus we need a high bias voltage to observe benzene by STM. Further, the bias voltage applied here is sharply discrete because we actually deal with a free molecule in our model calculations.

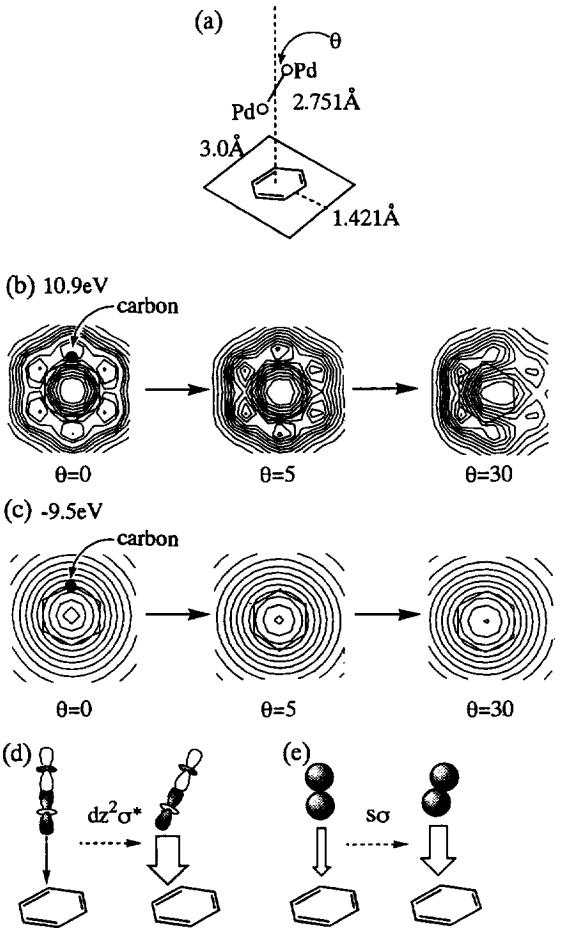

Fig. 2. The effect of tilting the Pd_2 tip on the benzene sample. Explanations for (a)–(e) are given in the text.

Next, we investigate the effect of tilting the tip on the benzene sample and the result is shown in Fig. 2. A similar study was also reported by Tsukada et al. [6,21] for different systems by a different method. The change in the calculated STM image by changing the tilting angle θ defined in Fig. 2a is exhibited in Figs. 2b and 2c. Fig. 2b shows the bias voltage of 10.9 eV, corresponding to the case of Fig. 1a, and Fig. 2c shows the bias voltage of -9.5 eV, corresponding to the case of Fig. 1c. When the tip is tilted, the position of the tip on the two-dimensional

sample surface is defined by the midpoint of Pd_2 as shown by the broken line in Fig. 2a. In Fig. 2b, the STM image is distorted as the tip is tilted, and the original C_6 symmetry disappears. However, in Fig. 2c the STM image is little affected by the tilting of the Pd_2 tip.

This difference is explained using Figs. 2d and 2e. The tip orbital responsible for this tunneling current is the $d_{z^2}\sigma^*$ orbital for Fig. 2b and the $5s\sigma$ orbital for Fig. 2c. The difference in the sensitivity to θ between these two cases is mainly due to the difference in these tip MOs. Because of the slenderness of the $d_{z^2}\sigma^*$ orbital, the orbital has high resolution and high sensitivity to the change in θ. When the tilting angle θ increases, the antibonding interaction of the benzene orbital with the $4d_{z^2}$ orbital of the outer Pd atom gradually increases, resulting in a decrease in the current on the right-hand side of the benzene sample. On the other hand, in the reverse flow, the $5s\sigma$ orbital has a spherical shape and the two 5s AOs have the same sign (bonding) as shown in Fig. 2e, so that the STM image does not depend sensitively on the angle θ. Moreover, the 5s orbital of Pd is more diffuse than the $4d_{z^2}$ orbital, so that the 5s orbital has a lower resolution than the $4d_{z^2}$ orbital. This example shows that the sensitivity to the tilting of the tip on the sample surface is understood from the nature of the MOs of the tip responsible for the STM current. It is not a simple function of the tip geometry but a function of the nodal character and the diffuseness of the responsible tip MO.

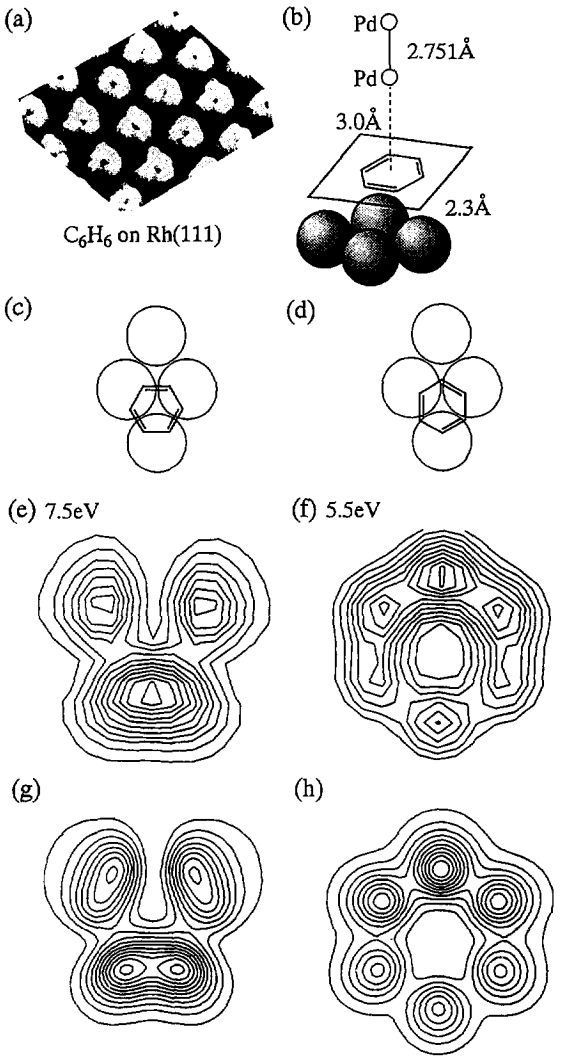

Fig. 3. (a) Experimental STM image of benzene adsorbed on a Rh (111) surface. (b) Calculational model, Pd_2 tip on C_6H_6/Ag_4 sample; (c) (e) (g) and (d) (f) (h) give two sets of adsorption geometry, the calculated STM image and MO density map.

4. Benzene adsorbed on a silver surface

The STM image of benzene adsorbed on a metal surface shows a characteristic feature. For example, the experimental STM image of benzene adsorbed on a Rh(111) surface shows only three peaks as exhibited in Fig. 3a [22]. To investigate the origin of such a characteristic image, we calculated the STM image of benzene adsorbed on a Ag_4 cluster using the Pd_2 tip (Fig. 3b).

There are two possible adsorbed structures of benzene on the threefold hollow site of the Ag(111) surface as shown in Figs. 3c and 3d. We calculated the STM image of each structure and the results are shown in Figs. 3e and 3f, respectively, which correspond to the lowest bias voltage, i.e. from the HOMO of Pd_2 to the LUMO and next-LUMO of C_6H_6/Ag_4. We assumed that the currents to the LUMO and next-LUMO occur with equal weight, since these orbitals are degenerate in the isolated system studied in the preceding section. This bias voltage applied here is lower than that applied in the calculation of benzene alone, because the energy level of the LUMO

and next-LUMO are lowered by the effect of the Ag_4 cluster. Fig. 3e shows a pattern similar to the experimental image, while Fig. 3f shows a different pattern. We therefore conclude that the structure (c) should be the real adsorbed structure observed by the experimental STM image. This result suggests the possibility of identifying the adsorbed structure by comparing the experimental and theoretical STM images.

Why is the STM image of benzene adsorbed on the metal surface different from that of benzene alone? We analyze this system by MO theory. First, we show a similarity between the STM map and the MO density map. The MO density maps shown in Figs. 3g and 3h were calculated as a sum of the LUMO and next-LUMO densities. Because the Pd $4d_{z^2}$ orbital of the tip does not have a node when it is vertical ($\theta = 0°$), the STM image reflects the density of the MO interacting with it, resulting in a similarity between them. If the tip orbital has a node along the sample plane, the STM image is very different from the orbital density as shown in Ref. [9]. We further note that the characteristic patterns of the STM image and the MO density shown in Figs. 3e and 3g, respectively, are due to the mixing of the HOMO and LUMO of (free) benzene caused by the interaction with the silver surface atoms.

5. Concluding remarks

The STM image reflects the local electronic structure of the tip–sample interacting system: the MOs in the HOMO–LUMO region of the tip and the sample responsible for the STM current are of particular importance. Further, we note that not only the interaction between the sample and the tip but also the interaction within the sample, for example, the interaction between adsorbate and surface, affects the STM image, because the latter interaction causes the redistribution and polarization of the responsible MOs. The site and structure of the adsorbate can be elucidated by a comparison of the experimental and theoretical STM images.

Acknowledgement

This study has been partially supported by a Grant-in-Aid for Scientific Research from the Japanese Ministry of Education, Science and Culture and by the New Energy and Industrial Technology Development Organization (NEDO).

References

[1] G. Binnig, H. Rohrer, Ch. Gerber and E. Weibel, Appl. Phys. Lett. 49 (1983) 57; 50 (1983) 120.
[2] R.S. Becker, J.A. Golovchenko and B.S. Swartzentruber, Nature 325 (1987) 419.
[3] D.M. Eigler and E.K. Schweizer, Nature 344 (1990) 524.
[4] J. Bardeen, Phys. Rev. Lett. 6 (1961) 57.
[5] M. Tsukada and N. Shima, J. Phys. Soc. Jpn. 56 (1987) 2875.
[6] M. Tsukada, K. Kobayashi, N. Isshiki and Y. Hasegawa, Surf. Sci. Rep. 13 (1991) 265.
[7] K. Hirose and M. Tsukada, Phys. Rev. Lett. 73 (1994) 150.
[8] K. Hirose and M. Tsukada, Phys. Rev. B 51 (1995) 5278.
[9] T. Fujita, H. Nakai and H. Nakatsuji, J. Chem. Phys. 104 (1996) 2410.
[10] J. Tersoff and D.R. Hamann, Phys. Rev. B 31 (1985) 805.
[11] N.D. Lang, Phys. Rev. Lett. 56 (1986) 1164; 58 (1987) 45.
[12] A. Farazdel and M. Dupuis, Phys. Rev. B 44 (1991) 3909.
[13] H. Ou-Yang, B. Kallebring and R.A. Marcus, J. Chem. Phys. 98 (1993) 7565.
[14] CRC handbook of chemistry and physics, 65th Ed. (Chemical Rubber, Cleveland, 1984/1985).
[15] A. Langseth and B.P. Stoicheff, Can. J. Phys. 34 (1956) 350.
[16] A.B. Anderson, M.R. McDevitt and F.L. Urbach, Surf. Sci. 146 (1984) 80.
[17] P.J. Hay and W.R. Wadt, J. Chem. Phys. 82 (1985) 299.
[18] S. Huzinaga, J. Chem. Phys. 42 (1965) 1293.
[19] T.H. Dunning Jr., J. Chem. Phys. 53 (1970) 2823.
[20] M. Dupuis and A. Farazdel, A MOTECC-91, Center for Scientific and Engineering Computations, IBM Corporation (1991).
[21] M. Tsukada, K. Kobayashi and N. Isshiki, Surf. Sci. 242 (1991) 12.
[22] H. Ohtani, R.J. Wilson, S. Chiang and C.M. Mate, Phys. Rev. Lett. 60 (1988) 2398.